

# Acid–Base Chemistry of a Carbenium Ion in a Zeolite under Equilibrium Conditions: Verification of a Theoretical Explanation of Carbenium Ion Stability

Weiguo Song,<sup>†</sup> John B. Nicholas,<sup>\*,‡</sup> and James F. Haw<sup>\*,†</sup>

Contribution from the Loker Hydrocarbon Research Institute and Department of Chemistry, University of Southern California, University Park, Los Angeles, California 90089-1661, and the Environmental Molecular Sciences Laboratory, Pacific Northwest National Laboratory, P.O. Box 999, Richland, Washington 99352

Received July 27, 2000

**Abstract:** The 1,3-dimethylcyclopentenyl carbenium ion ( $C_7H_{11}^+$ ) was reproducibly prepared on zeolite HZSM-5 using a pulse-quench reactor, and then each of a number of bases was coadsorbed into the catalyst channels to either compete with the cation for protonation or to possibly react with it as a nucleophile. For seven bases with proton affinities (PA) between 142 and 212.1 kcal/mol, there was no reaction with  $C_7H_{11}^+$ . Coadsorption of smaller amounts of dimethylacetamide (PA = 217 kcal/mol) also produced no reaction, but with a higher loading, a proton was transferred from the carbenium ion to the base to leave 1,3-dimethylcyclopenta-1,3-diene in the zeolite as a neutral olefin. Deprotonation was the primary reaction with coadsorption of either pyridine (PA = 222 kcal/mol) or trimethylphosphine (PA = 229.2 kcal/mol). The estimated experimental deprotonation enthalpy for  $C_7H_{11}^+$ , ~217 kcal/mol in the zeolite, is in excellent agreement with MP4/6-311G\* gas-phase value of 215.6 kcal/mol. Coadsorption of either  $NH_3$  (PA = 204.0 kcal/mol) or  $PH_3$  (PA = 188 kcal/mol) does not deprotonate the carbenium ion, but these species do react as nucleophiles to form onium ion derivatives of  $C_7H_{11}^+$ . Analogous onium complexes with pyridine or trimethylphosphine formed in lower yields due to steric constraints in the zeolite channels. The essential experimental observations were all predicted and explained by density functional calculations (B3LYP/6-311G\*\*) and extensions of our recently developed theory of carbenium ion stability in zeolites. In addition, we report theoretical geometries for several complexes which contain unusual C–H...X hydrogen bonds.

Acid–base chemistry in the solution and gas phases is well understood in terms of quantitative thermodynamic properties such as acid dissociation constants and deprotonation energies. In the gas or solution phases, there are three general reactions between an acid AH and a base B: (1) formation of a hydrogen-bonded<sup>1</sup> complex without proton transfer, AH...B; (2) formation of a zwitterionic  $A^-\cdots HB^+$  complex that is stabilized by Coulombic interactions and hydrogen bonding; or (3) formation of a covalently bound onium ion<sup>2</sup> complex. The application of thermodynamic principles to acid–base reactions on solid surfaces—most importantly those used in heterogeneous catalysis—is far less clear than for the solution and gas phases. One concern is the possibility that adsorption of acids or bases onto a solid surface may not be sufficiently reversible for thermodynamic equilibrium to be established.

The most important and most studied solid acids are aluminosilicate zeolites, which are microcrystalline and have well-defined pore systems. Of particular interest are the acid–base reactions of hydrocarbons on zeolites. Ethylene, propene and other simple olefins have been shown to form neutral, weakly hydrogen-bonded complexes with Brønsted sites in zeolites, for example, **1**.<sup>3</sup> A similar complex is formed with benzene. For

the case of propene, it is well established that proton transfer can occur in concert with a nucleophilic attack by an oxygen of the conjugate base of the zeolite Brønsted site. This reaction produces a kind of oxonium ion that is called a framework-bound alkoxy species in the zeolite literature, for example, **2**.<sup>4</sup> The protonated forms of unsaturated hydrocarbons are carbenium ions.

Over the last several years we have developed energetic criteria for the formation of stable carbenium species in zeolites.<sup>5</sup> Simply put, we find that for a stable carbenium ion to form on a given zeolite the proton affinity (PA) of the parent olefin must be greater than a certain threshold. In our previous work we used a combination of MP4(SDTQ)/6-311G\* calculations and experimental data to establish the threshold at approximately 209.0 kcal/mol for olefins and aromatics in HZSM-5.<sup>5</sup> It is important to understand this threshold in context: the proton affinities of propene, hexamethylbenzene, and pyridine are 179.6, 205.7, and 222 kcal/mol, respectively. Clearly, only exceptionally basic hydrocarbons will react exothermically with a zeolite Brønsted site in an elementary reaction to form a persistent carbenium ion. One of the three persistent carbenium ions identified in our earlier work<sup>4,6,7</sup> was the 1,3-dimethylcyl-

<sup>†</sup> University of Southern California.

<sup>‡</sup> Pacific Northwest National Laboratory.

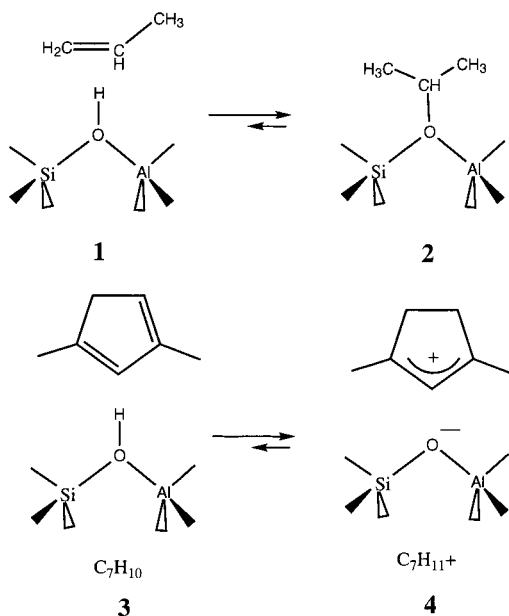
(1) Jeffrey, G. A. *An Introduction to Hydrogen Bonding*; Oxford University Press: New York, 1997.

(2) Olah, G. A.; Laali, K.; Wang, Q.; Prakash, G. K. S. *Onium Ions*; John Wiley and Sons: New York, 1998.

(3) White, J. L.; Beck, L. W.; Haw, J. F. *J. Am. Chem. Soc.* **1992**, *114*, 6182–6189.

(4) Haw, J. F.; Richardson, B. R.; Oshiro, I. S.; Lazo, N. L.; Speed, J. A. *J. Am. Chem. Soc.* **1989**, *111*, 2052–2058.

(5) Nicholas, J. B.; Haw, J. F. *J. Am. Chem. Soc.* **1998**, *120*, 11804–11805.



clopentenyl cation (**4**,  $C_7H_{11}^+$ ), which could in principle be formed by protonation of 1–3-dimethylcyclopent-1,3-diene (**3**,  $C_7H_{10}$ ,  $PA = 215.6$  cal/mol). Note that the  $C_7H_{11}^+$  cation does *not* form an oxonium (alkoxy) species with the framework of the zeolite—analogue to **2**. Our theoretical work suggests this is due to steric constraints imposed by the topology of the zeolite channel.<sup>8</sup>

We were led to the present work by a prediction developed from our previous theoretical study<sup>5</sup>—that once formed, the  $C_7H_{11}^+$  cation could act as an acid and deprotonate to form the parent diene when presented with a coadsorbed base molecule having a proton affinity greater than  $\sim 216$  kcal/mol, the deprotonation enthalpy of  $C_7H_{11}^+$ . By analogy to acid–base reactions in other media, the reaction of the  $C_7H_{11}^+$  cation with a coadsorbed base could have three outcomes: (1) no reaction beyond hydrogen-bonding of the base to the carbenium ion, giving  $C_7H_{11}^+ \cdots B$ , (2) deprotonation of the carbenium ion by the base to form a hydrogen-bonded complex between the neutral hydrocarbon and protonated base,  $C_7H_{10} \cdots H:B^+$ , or (3) formation of an onium ion complex between the carbenium ion and added base ( $C_7H_{11}B^+$ ). Implicit in this prediction is the requirement that the acid–base reactions of carbenium ions in zeolites are sufficiently reversible for the application of thermodynamics. Furthermore, since our predictions are based on gas-phase thermodynamic quantities, quantitative agreement with experiment would require that these not be strongly altered by the zeolite environment.

To test out theoretical predictions, we reproducibly prepared samples of the  $C_7H_{11}^+$  cation in zeolite HZSM-5 (2 s of reaction at 573 K) using a pulse-quench reactor<sup>7–11</sup> and ethylene-<sup>13</sup>C<sub>2</sub> as a convenient starting material. <sup>13</sup>C solid-state NMR was used to observe the reaction products obtained upon adsorption (usually at 298 K) of a number of base molecules. These

coadsorbed bases covered a range of proton affinities<sup>12</sup> between 142.0 kcal/mol (carbon monoxide) to 229.2 kcal/mol (trimethylphosphine), allowing us to effectively “titrate” the  $C_7H_{11}^+$  acid. When the formation of  $C_7H_{10} \cdots H:B^+$  complexes was theoretically predicted to be energetically favored over the initial state,  $C_7H_{11}^+ \cdots B$ , we observed deprotonation of the carbenium ion to form the neutral parent olefin in the zeolite. Deprotonation of  $C_7H_{11}^+$  did not occur when the  $C_7H_{10} \cdots H:B^+$  complex was predicted to be higher in energy than the corresponding  $C_7H_{11}^+ \cdots B$  complex. In addition,  $C_7H_{11}^+$  formed an ammonium ion or phosphonium ion when the weak bases  $NH_3$  or  $PH_3$  were coadsorbed. In these cases theory predicted the onium ion to be the most stable of the three possible states. In several cases some of the three possible states were not found to be theoretically stable. Experimental observations verified these predictions. For example, oxonium ion formation did not occur with water or dimethyl ether. Neither did CO bind to  $C_7H_{11}^+$  in the zeolite to form an acylium ion. Theory also predicted that pyridine and trimethylphosphine would preferentially form onium ions. Indeed, these were observed experimentally as minority products. However, steric constraints in the zeolite channel work against onium ion formation in the cases of these bulky bases, and deprotonation is the dominant reaction observed. This work provides an important extension and verification of our previously proposed theory<sup>5</sup> of carbenium ion stability in zeolites.

## Experimental Section

**Materials and Regents.** All results reported were obtained on a pelletized catalyst composed of 70 wt % zeolite HZSM-5 with a Si/Al ratio of 19 and 30% alumina binder. Ethylene-<sup>13</sup>C<sub>2</sub> (99% <sup>13</sup>C), acetone-2-<sup>13</sup>C (99% <sup>13</sup>C), and pyridine-<sup>15</sup>N (99% <sup>15</sup>N) were purchased from Isotec. Phosphine gas and all other reagents were purchased from Aldrich. **Safety Note:** Phosphine gas is toxic and spontaneously flammable in air.

**Preparation of the  $C_7H_{11}^+$  Cation in Zeolite HZSM-5.** We used a pulse-quench reactor<sup>8–11</sup> to synthesize the cation on the zeolite. For each sample, 0.63 mmol of ethylene-<sup>13</sup>C<sub>2</sub> was pulsed onto the catalyst at 573 K and allowed to react for 2 s prior to a thermal quench to room temperature. The major products of the reaction of ethylene are propene, butenes, isobutane, and isopentane; these volatile products exit the catalyst before the quench. A small, but reproducible amount of the  $C_7H_{11}^+$  cation remains on the catalyst as the major adsorbed organic species. NMR spin counting indicates that, for the catalyst and conditions used, the yield of the  $C_7H_{11}^+$  cation corresponds to 1–4% of the acid sites.<sup>8</sup>

After each sample was quenched, the reactor was sealed off and transferred into a glovebox filled with nitrogen. Typically, the catalyst pellets were then transferred into a 7.5 mm MAS rotor which was sealed with a Kel-F end-cap, and <sup>13</sup>C MAS NMR spectra were acquired then to establish the presence of the  $C_7H_{11}^+$  cation prior to coadsorption of a base. The MAS rotor was then returned to the glovebox and opened. The catalyst pellets were transferred to a shallow bed CAVERN device<sup>13–15</sup> which was attached to a vacuum line and evacuated for 30 min. The base was then adsorbed at room temperature, with the exception of acetone, which was introduced at 193 K to prevent oligomerization. The amount of base used is expressed in units of equivalents (equiv) relative to the number of Brønsted acid sites in the sample. Typical loadings were  $\sim 2$  equiv to ensure that the zeolite acid sites were completely titrated and excess base was available for reaction with the  $C_7H_{11}^+$  cation.

(12) The experimental proton affinity values reported here are the most recent values or the values with the smallest uncertainties listed in the NIST Chemistry WebBook (<http://webbook.nist.gov/chemistry/>).

(13) Xu, T.; Haw, J. F. *Top. Catal.* **1997**, *4*, 109–118.

(14) Munson, E. J.; Murray, D. K.; Haw, J. F. *J. Catal.* **1993**, *141*, 733–736.

(15) Haw, J. F.; Nicholas, J. B.; Xu, T.; Beck, L. W.; Ferguson, D. B. *Acc. Chem. Res.* **1996**, *29*, 259–267.

(6) Xu, T.; Haw, J. F. *J. Am. Chem. Soc.* **1994**, *116*, 7753–7759.

(7) Xu, T.; Barich, D. H.; Goguen, P. W.; Song, W.; Wang, Z.; Nicholas, J. B.; Haw, J. F. *J. Am. Chem. Soc.* **1998**, *120*, 4025–4026.

(8) Haw, J. F.; Nicholas, J. B.; Song, W.; Deng, F.; Wang, Z.; Heneghan, C. S. *J. Am. Chem. Soc.* **2000**, *122*, 4763–4775.

(9) Haw, J. F.; Goguen, P. W.; Xu, T.; Skloss, T. W.; Song, W.; Wang, Z. *Angew. Chem.* **1998**, *37*, 948–949.

(10) Goguen, P. W.; Xu, T.; Barich, D. H.; Skloss, T. W.; Song, W.; Wang, Z.; Nicholas, J. B.; Haw, J. F. *J. Am. Chem. Soc.* **1998**, *120*, 2651–2652.

(11) Barich, D. H.; Xu, T.; Song, W.; Wang, Z.; Deng, F.; Haw, J. F. *J. Phys. Chem. B* **1998**, *102*, 7163–7168.

**Table 1.** Experimental and Theoretical (B3LYP/6-311G\*) Proton Affinities ( $\Delta H$ ), Theoretical Methyl Cation Affinities ( $\Delta H$ ), and Theoretical Energies of the Three Possible Adsorption Complexes Relative to the Sum of the Total Energies of Isolated  $C_7H_{11}^+$  and the Co-Adsorbate ( $\Delta E$ )<sup>a</sup>

Co-adsorbate	proton affinity		CH <sub>3</sub> <sup>+</sup> affinity	relative energies		
	exp.	theory	theory	$C_7H_{11}^+ - :B$	$C_7H_{10} - :HB^+$	$(C_7H_{11}B)^+$
CO	142	135.0	78.6	-2.2		10.2
H <sub>2</sub> O	165	169.8	73.9	-12.6		
nitromethane	180.4	176.8	82.8	-13.2		
PH <sub>3</sub>	188	185.1	102.2	-4.0	21.0	-4.3
DME	189	187.7	88.2	-10.3		
acetone	194	193.1	93.0	-13.1		
NH <sub>3</sub>	204.0	207.8	109.1	-12.2	-6.6	-19.3
DMFA	212.1	208.4	106.2	-17.6	-6.3	-17.0
DMA	217.0	215.6	109.8	-16.6	-8.0	-13.3
pyridine	222	223.4	123.6	-11.1	-15.0	-22.9
TMP	229.2	225.2	137.7	-8.1	-10.0	-31.1

<sup>a</sup> All values in kcal/mol. Deprotonation enthalpy of  $C_7H_{11}^+$  is 222.4 kcal/mol at B3LYP/6-311G\*.

**NMR Spectroscopy.** <sup>13</sup>C, <sup>15</sup>N, and <sup>31</sup>P solid-state NMR experiments were performed with magic angle spinning (MAS) on a modified Chemagnetics CMX-300 MHz spectrometer operating at 75.4 MHz for <sup>13</sup>C, 30.4 MHz for <sup>15</sup>N and 121.3 MHz for <sup>31</sup>P. Hexamethylbenzene (17.4 ppm), glycine-<sup>15</sup>N (-347.6 ppm), and 85% H<sub>3</sub>PO<sub>4</sub> (0 ppm) were used as external chemical shift standards for <sup>13</sup>C, <sup>15</sup>N, and <sup>31</sup>P, respectively. <sup>13</sup>C chemical shifts are reported relative to TMS, <sup>15</sup>N chemical shifts relative to nitromethane, and <sup>31</sup>P chemical shifts relative to 85% H<sub>3</sub>PO<sub>4</sub>. Chemagnetics-style pencil probe spun 7.5 mm zirconia rotors at 6.5 kHz with active spin speed control ( $\pm 3$  Hz). Typical NMR experiments included: cross polarization (CP, contact time = 2 ms, pulse delay = 1 s, 4000 scans); cross polarization with interrupted decoupling (contact time = 2 ms, pulse delay = 1 s, 4000 scans, dipolar dephasing time = 50  $\mu$ s); single pulse excitation with proton decoupling (Bloch decay, pulse delay = 10 s, 4000 scans). All spectra shown were obtained at room temperature using cross polarization, except where otherwise stated.

**Theoretical Methods.** We optimized the geometries of all of the coadsorbate base molecules, their protonated and methylated analogues, and all possible complexes formed between the bases and  $C_7H_{11}^+$ . We calculated the vibrational frequencies for the bases, protonated bases, and methylated bases, to obtain estimates of the enthalpies of protonation (proton affinities) and methylation (methyl cation affinities). The deprotonation enthalpy of  $C_7H_{11}^+$  was also calculated. We did not obtain frequencies for the larger complexes, as the relative energies were sufficient to predict the behavior observed experimentally. All of the optimizations and frequency calculations were done using density functional theory (DFT) at the B3LYP/6-311G\* level<sup>16,17</sup> as implemented in Gaussian98.<sup>18</sup> We obtained the <sup>13</sup>C isotropic chemical shifts of  $C_7H_{11}^+$  and its parent olefin  $C_7H_{10}$  from GIAO-MP2<sup>19</sup> calculations with a tzp basis set on C and a dz basis set on H.<sup>20</sup> We used the B3LYP/6-311G\* optimized geometries for the GIAO calculations. The reported chemical shifts are relative to those obtained for TMS at the same level of theory. The GIAO-MP2 calculations were done with ACES-II.<sup>21</sup>

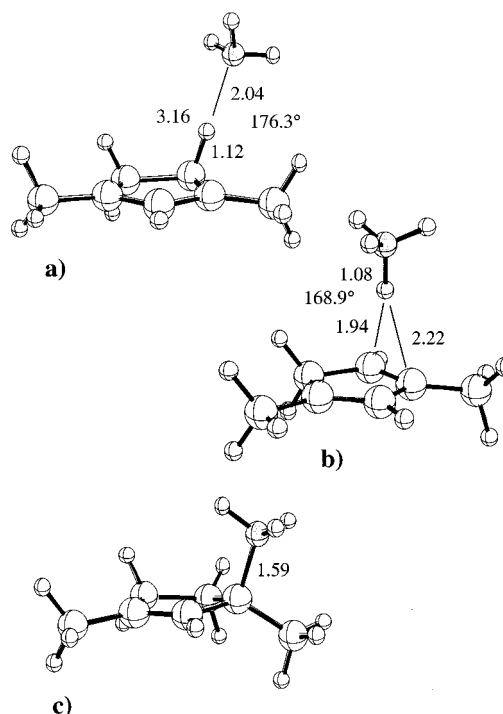


**Figure 1.** B3LYP/6-311G\* optimized geometries for possible complexes formed by  $C_7H_{11}^+$  and  $NH_3$ : (a) the  $C_7H_{11}^+ - -NH_3$  hydrogen-bonded complex; (b) the  $C_7H_{10} - -HNH_3^+$  hydrogen-bonded complex; (c) the covalently bound ammonium ion,  $C_7H_{11}NH_3^+$ .

## Results

**Theoretical.** The 11 basic coadsorbates we used are listed in Table 1. The geometries of the isolated molecules and their protonated analogues are unremarkable and will not be presented. However, the complexes formed between the bases and  $C_7H_{11}^+$  are significantly more interesting. We show in Figure 1, as a representative example, optimized geometries for the three complexes involving  $NH_3$ . In Figure 1a we show the hydrogen-bonded complex between  $NH_3$  and  $C_7H_{11}^+$ . Nitrogen coordinates to the most acidic hydrogen of  $C_7H_{11}^+$ . The C–H distance is 1.12 Å, 0.02 Å longer than it is in the isolated carbenium ion calculated at the same level of theory. The H–N distance is 2.04 Å, the C–N distance is 3.16 Å, and the C–H–N angle is 176.3°. All of these parameters are consistent with a strong hydrogen bond, as is the hydrogen-bonding energy of

(16) Becke, A. D. *J. Chem. Phys.* **1993**, *98*, 5648–5652.

(17) Hehre, W. J.; Radom, L.; Schleyer, P. v. R.; Pople, J. A. *Ab Initio Molecular Orbital Theory*; John Wiley & Sons: New York, 1986.

(18) Frisch, M. J.; Trucks, G. W.; Schlegel, H. B.; Scuseria, G. E.; Robb, M. A.; Cheeseman, J. R.; Zakrzewski, V. G.; Montgomery, J. A., Jr.; Stratmann, R. E.; Burant, J. C.; Dapprich, S.; Millam, J. M.; Daniels, A. D.; Kudin, K. N.; Strain, M. C.; Farkas, O.; Tomasi, J.; Barone, V.; Cossi, M.; Cammi, R.; Mennucci, B.; Pomelli, C.; Adamo, C.; Clifford, S.; Ochterski, J.; Petersson, G. A.; Ayala, P. Y.; Cui, Q.; Morokuma, K.; Malick, D. K.; Rabuck, A. D.; Raghavachari, K.; Foresman, J. B.; Cioslowski, J.; Ortiz, J. V.; Stefanov, B. B.; Liu, G.; Liashenko, A.; Piskorz, P.; Komaromi, I.; Gomperts, R.; Martin, R. L.; Fox, D. J.; Keith, T.; Al-Laham, M. A.; Peng, C. Y.; Nanayakkara, A.; Gonzalez, C.; Challacombe, M.; Gill, P. M. W.; Johnson, B. G.; Chen, W.; Wong, M. W.; Andres, J. L.; Head-Gordon, M.; Replogle, E. S.; Pople, J. A. *Gaussian 98*, revision A.4; Gaussian, Inc.: Pittsburgh, PA, 1998.

(19) Gauss, J. *Chem. Phys. Lett.* **1992**, *191*, 614–620.

(20) Schäfer, A.; Horn, H.; Ahlrichs, R. *J. Chem. Phys.* **1992**, *97*, 2571–2577.

(21) Stanton, J. F.; Gauss, J.; Watts, J. D.; Lauderdale, W. J.; Bartlett, R. J. *ACES II*, an ab initio quantum chemical program system.

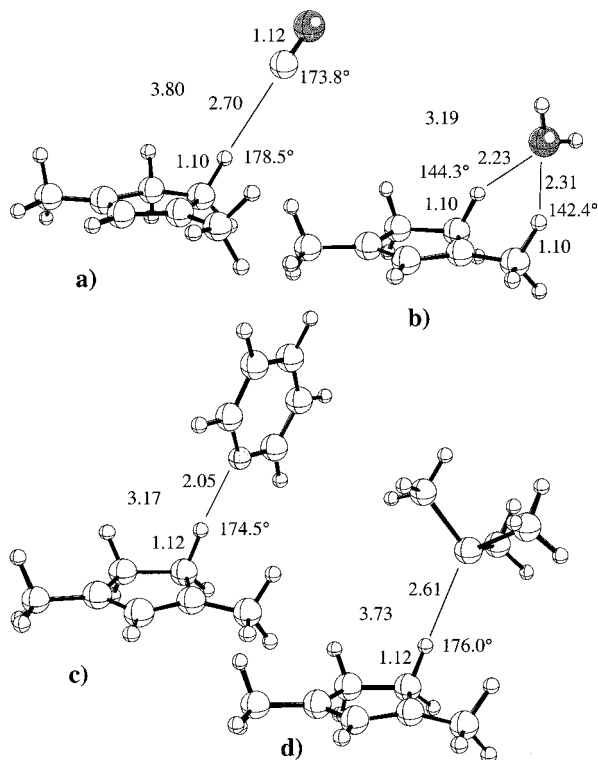


**Figure 2.** B3LYP/6-311G\* optimized geometries for  $C_7H_{11}^+ \cdots B$  hydrogen-bonded complexes involving: (a) CO, (b)  $H_2O$ , (c) pyridine (Py), and (d)  $P(CH_3)_3$ .

−12.2 kcal/mol. The C–H–N angle is  $176.3^\circ$ , very close to linear. Figure 1b shows the optimized geometry for the  $C_7H_{10} \cdots NH_4^+$  complex. In this case the acidic ammonium proton interacts with both of the carbons of the double bond in an asymmetric fashion; the C–H distances are 1.94 and 2.22 Å. The N–H bond is 1.08 Å, 0.06 Å longer than that calculated for isolated  $NH_4^+$ , and the C–N distance is 3.01 Å, 0.15 Å shorter than that in the  $C_7H_{11}^+ \cdots NH_3$  complex. The C–H–N angle is  $168.9^\circ$ , still close to linear. The geometry suggests the strong tendency for ammonium to donate the proton back to the olefin, regenerating the complex shown in Figure 1a. The hydrogen bonding energy in this case is −6.6 kcal/mol. Finally, Figure 1c shows the corresponding covalent ammonium ion complex, in which nitrogen is bonded to carbon. The optimized N–C bond length of 1.59 Å compares to a value of 1.52 Å calculated for  $CH_3-NH_3^+$ . This is the lowest energy of the three possible states, being −19.3 kcal/mol below the sum of the total energies of isolated  $NH_3$  and  $C_7H_{11}^+$ . In contrast to  $NH_3$ , stable geometries for all three types of complexes involving some of the other bases could not be obtained.

Figure 2 shows the geometries of several of the other  $C_7H_{11}^+ \cdots B$  hydrogen-bonded complexes. Figure 2a shows the complex formed between CO and  $C_7H_{11}^+$ . The C–H bond distance is 1.10 Å, and H–C distance is 2.70 Å, and the C–O triple bond length is 1.12 Å. The bonding arrangement is almost linear, with C–H–C and H–C–O angles of  $178.5^\circ$  and  $173.8^\circ$ . The corresponding C–C distance is 3.80 Å. In contrast to CO, all of the complexes in which the base molecule interacts with the carbenium ion through an oxygen give geometries with bifurcated hydrogen bonds, involving both the oxygen lone pairs. The complex formed between  $C_7H_{11}^+$  and  $H_2O$  is given as an example in Figure 2b. The bonding arrangement is somewhat asymmetric, with H–O hydrogen-bonding distances of 2.23 and 2.31 Å. The bifurcated nature of the interaction results in

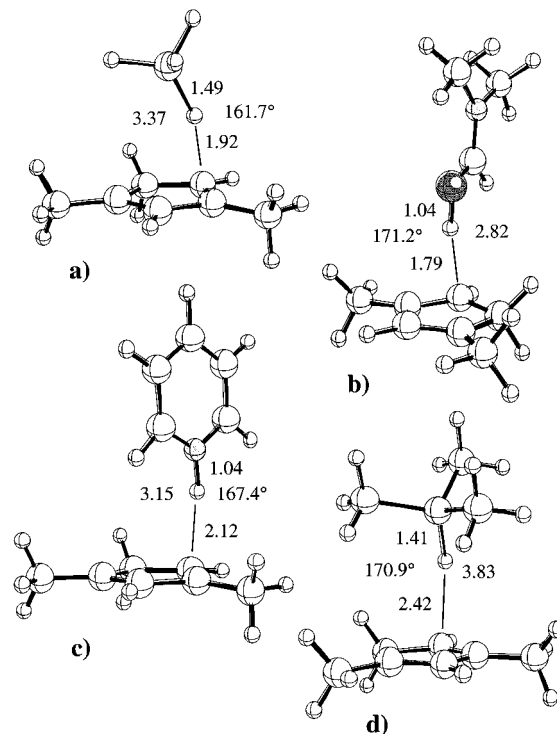


**Figure 3.** B3LYP/6-311G\* optimized geometries for  $C_7H_{10} \cdots H-B^+$  hydrogen-bonded complexes involving: (a)  $PH_3$ , (b) DMF, (c) Py, and (d)  $P(CH_3)_3$ .

C–H–O angles that are far from linear:  $144.3^\circ$  and  $142.4^\circ$ . The closest C–O distance is 3.19 Å. It is somewhat surprising that the oxygen prefers to interact with one of the acidic and one of the methyl hydrogens of the carbenium ion, rather than interacting with the two, symmetry-equivalent, acidic hydrogens. Whereas we can optimize a stable complex with that hydrogen bonding geometry (not shown), it is 1.1 kcal/mol higher in energy than that of the geometry in Figure 2b.

Nitromethane, dimethyl ether (DME), acetone, dimethylformamide (DMF), and dimethylacetamide (DMA) also all form bifurcated hydrogen-bonded complexes (not shown) similar to that for  $H_2O$  (Figure 2b). The H–O distances in the DME and acetone complexes are within  $\sim 0.05$  Å of the H–O distances in the  $C_7H_{10}^+ \cdots H_2O$  complex. The more basic DMF and DMA complexes tend to bond more strongly to the acidic proton, resulting in H–O distances of 2.14 and 2.32 Å (DMF) and 2.14 and 2.26 Å (DMA). Pyridine forms a hydrogen-bonded complex (Figure 2c) very similar to that formed by  $NH_3$ . The C–H, H–N, and C–N distances are all within 0.01 Å of those in  $C_7H_{11}^+ \cdots NH_3$ , and the C–H–N angle ( $174.5^\circ$ ) is only  $\sim 2^\circ$  farther from linear. Last, both  $PH_3$  and trimethylphosphine ( $P(CH_3)_3$ ) form hydrogen bonds with the acidic proton. Figure 2d shows the optimized geometry of the  $C_7H_{11}^+ \cdots P(CH_3)_3$  complex. The P–H distance in the  $P(CH_3)_3$  complex is 2.61 Å, whereas it is 2.90 Å for  $C_7H_{11}^+ \cdots PH_3$ , reflecting the fact that  $PH_3$  is much less basic than  $P(CH_3)_3$ . Similarly, the C–H bond shows some lengthening in the  $P(CH_3)_3$  complex (1.12 Å), whereas it is 1.10 Å in the  $PH_3$  complex. In both cases the C–H–P bond angles are close to linear;  $176.0^\circ$  for  $P(CH_3)_3$ , and  $177.5^\circ$  for  $PH_3$ .

The optimized geometries of some of the other  $C_7H_{10} \cdots H-B^+$  complexes are shown in Figure 3. These complexes exhibit  $\pi$ -cation interactions between the acidic hydrogen of the protonated bases and the olefin double bond. Figure 3a shows that the acidic hydrogen of  $PH_4^+$  coordinates primarily with

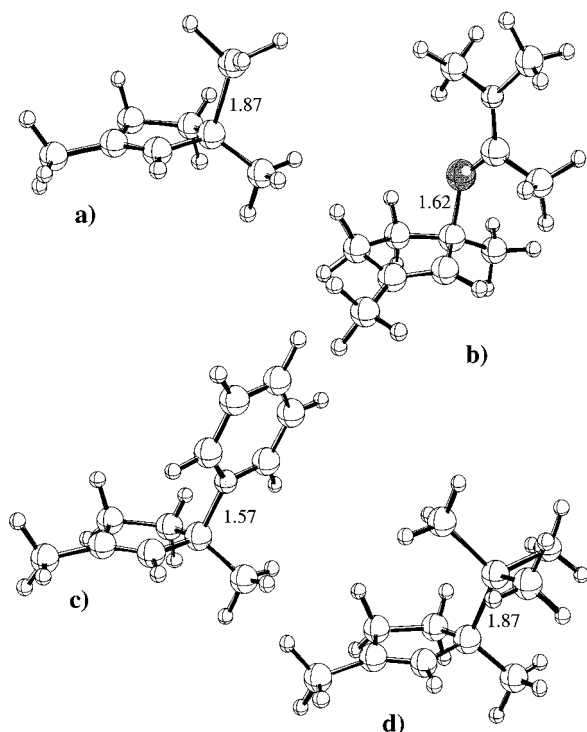


**Figure 4.** B3LYP/6-311G\* optimized geometries for onium ions formed by: (a)  $\text{PH}_3$ , (b) DMA, (c) Py, and (d)  $\text{P}(\text{CH}_3)_3$ .

one carbon of the olefin, giving an optimized H–C distance of 1.92 Å. The other H–C distance is 2.21 Å. The P–H bond length of 1.49 Å is considerably longer than the value of 1.40 Å in isolated  $\text{PH}_4^+$  calculated at the same level of theory. The primary P–H–C angle of 161.7° results in a P–C distance of 3.37 Å. Overall the geometry suggests the pending transfer of the proton back to the olefin. Indeed, the energy of this state is much higher than that of the isolated carbenium ion and neutral base (+21.0 kcal/mol, Table 1). There is evidently some energetic barrier that prevents spontaneous transfer of the proton to the olefin. In contrast, formation of the complex between the olefin and  $\text{P}(\text{CH}_3)_3\text{H}^+$  (Figure 3d) is exothermic, due to the much greater basicity of  $\text{P}(\text{CH}_3)_3$ . Thus, the P–H bond length of 1.41 Å is much closer to that in isolated  $\text{P}(\text{CH}_3)_3\text{H}^+$  (1.40 Å).  $\text{P}(\text{CH}_3)_3\text{H}^+$  is also much farther from the olefin, with a H–C distances of 2.42 and 2.50 Å, and a P–C distance of 3.83 Å. The primary P–H–C angle is 170.9°. Both DMF (Figure 4b) and DMA (not shown) form stable complexes in which the base is protonated. These complexes have the shortest H–C distances, with values of 1.79 and 2.19 Å for DMF and 1.97 and 2.32 Å for DMA. These distances reflect the fact that DMA is more basic than DMF. The O–H bond distance of 1.04 Å (DMF) and 1.01 Å (DMA) also indicate the  $\text{DMAH}^+$  cation is more stable and less prone to giving the proton back to the olefin. The resulting O–C distances are 2.82 Å (DMF) and 2.92 Å (DMA), with corresponding O–H–C angles of 171.2° and 155.2°. Finally, formation of a  $\text{C}_7\text{H}_{10}^- \cdots \text{H}:\text{Py}^+$  complex (Figure 4c) is also exothermic. The H–C distances of 2.12 and 2.28 Å are longer than the corresponding distances in the  $\text{NH}_3$  complex (1.94 and 2.22 Å), consistent with the greater basicity of pyridine. Similarly, the H–N bond distance of 1.04 Å is shorter than the 1.08 Å obtained for  $\text{NH}_3$ . The C–N distance is 3.15 Å, 0.14 Å longer than calculated the  $\text{NH}_3$  complex.

In Figure 4 we present the optimized geometries for some of the other onium ions. Although formation of the  $\text{C}_7\text{H}_{11}\text{P}(\text{CH}_3)_3^+$  onium ion (Figure 4d) is much more exothermic than that of

the  $\text{C}_7\text{H}_{11}\text{PH}_3^+$  ion (Figure 4a), both have C–P bond lengths of 1.87 Å. These bond lengths compare to calculated values of 1.81 Å in isolated  $\text{CH}_3\text{PH}_3^+$  and  $\text{P}(\text{CH}_3)_4^+$ . This is in agreement with the much weaker attraction of these bases for  $\text{C}_7\text{H}_{11}^+$  ( $\Delta H = -4.3$  and  $-31.1$  kcal/mol) versus  $\text{CH}_3^+$  ( $\Delta H = -102.2$  and  $-137.7$  kcal/mol). The C–O bond distance in the  $\text{C}_7\text{H}_{11}\text{DMA}^+$  ion (Figure 4b) is 1.62 Å, whereas it is 1.64 Å in the  $\text{C}_7\text{H}_{11}\text{DMF}^+$  ion (a very similar geometry which is not shown). These bond distances compare to values of 1.46 Å in isolated  $\text{CH}_3\text{DMF}^+$  and  $\text{CH}_3\text{DMA}^+$ . Finally, the  $\text{C}_7\text{H}_{11}\text{Py}^+$  onium ion (Figure 4c) gives an optimized C–N bond length of 1.57 Å, which corresponds to 1.59 Å in the  $\text{C}_7\text{H}_{11}\text{NH}_3^+$  ion (Figure 1c). For comparison, the C–N bonds in isolated  $\text{CH}_3\text{NH}_3^+$  and  $\text{CH}_3\text{Py}^+$  are shorter at 1.52 and 1.48 Å, again reflecting the higher affinity of the bases for  $\text{CH}_3^+$  ( $\Delta H = -109.1$  and  $-137.7$  kcal/mol) versus  $\text{C}_7\text{H}_{11}^+$  ( $\Delta H = -19.3$  and  $-31.1$  kcal/mol).

Table 1 gives the experimental and theoretical proton affinities for all of the coadsorbed bases as well as the calculated deprotonation enthalpy for  $\text{C}_7\text{H}_{11}^+$  (for which no experimental data is available). The B3LYP/6-311G\* level of theory does a reasonable job of predicting the proton affinities of the coadsorbed bases. Generally the theoretical values are within 4 kcal/mol of experiment, although the proton affinity of CO is significantly underestimated. The deprotonation enthalpy of  $\text{C}_7\text{H}_{11}^+$  is probably considerably overestimated at the B3LYP/6-311G\* level, which we will discuss below. Table 1 also gives the energy of complex formation between the coadsorbates and  $\text{C}_7\text{H}_{11}^+$ . If we first consider the theoretical values, we find that only pyridine and  $\text{P}(\text{CH}_3)_3$  have proton affinities greater than the deprotonation enthalpy of  $\text{C}_7\text{H}_{11}^+$ . As expected, for only these two coadsorbates is the  $\text{C}_7\text{H}_{10}^- \cdots \text{H}:\text{B}^+$  complex lower in energy than the  $\text{C}_7\text{H}_{11}^+ \cdots \text{B}$  complex. Thus, we predict that these are the only two coadsorbates for which it might be possible to experimentally observe deprotonation of the carbenium ion and formation of the olefin. For all other coadsorbates the  $\text{C}_7\text{H}_{11}^+ \cdots \text{B}$  complex is energetically preferred. For several of the coadsorbates (CO,  $\text{H}_2\text{O}$ , DME, and acetone) no  $\text{C}_7\text{H}_{10}^- \cdots \text{H}:\text{B}^+$  complex can even be obtained theoretically. Attempts at optimization of these  $\text{C}_7\text{H}_{10}^- \cdots \text{H}:\text{B}^+$  complexes all revert to  $\text{C}_7\text{H}_{11}^+ \cdots \text{B}$  complexes during the course of the calculation.

If we instead consider the experimental proton affinity data, there appears to be a small discrepancy—the experimental proton affinity of pyridine (222 kcal/mol) is lower, rather than higher, than the B3LYP/6-311G\* deprotonation enthalpy of  $\text{C}_7\text{H}_{11}^+$  (222.6 kcal/mol). However, the problem here is simply that the B3LYP/6-311G\* level of theory does not do a good job of estimating the deprotonation enthalpy of  $\text{C}_7\text{H}_{11}^+$ . We have found this deficiency with the B3LYP functional in predicting the proton affinities of olefins in general. Calculation of the deprotonation enthalpy at the more accurate MP4(sdtq)/6-311G\* level gives a value of 215.6 kcal/mol,<sup>5</sup> which eliminates the discrepancy and is entirely in line with our prediction of a stable  $\text{C}_7\text{H}_{10}^- \cdots \text{H}:\text{Py}^+$  complex.

In addition to the equilibria discussed above, there is also the possibility that the coadsorbate will react with  $\text{C}_7\text{H}_{11}^+$  to form a stable onium ion. From Table 1 we see that the theoretical results predict onium ions can form for all coadsorbates except  $\text{H}_2\text{O}$ , DME, and acetone. For CO an onium ion can be optimized, but its formation is highly endothermic and can thus be ignored. In four cases ( $\text{PH}_3$ ,  $\text{NH}_3$ , Py, and  $\text{P}(\text{CH}_3)_3$ ), the onium ion is the energetically preferred state. Whereas the difference in energy between the  $\text{C}_7\text{H}_{11}^+ \cdots \text{B}$  complex and the onium ion is small for  $\text{PH}_3$ , it is possible that both species will be observed. However, for  $\text{NH}_3$ , Py, and  $\text{P}(\text{CH}_3)_3$  the onium

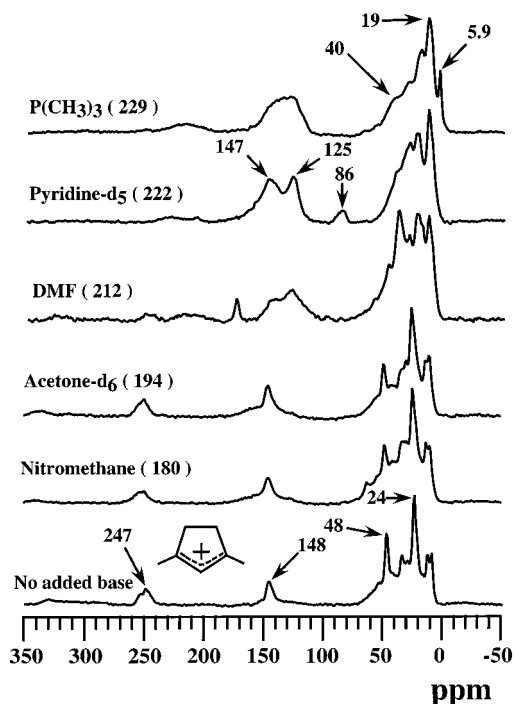


**Figure 5.**  $^{13}\text{C}$  CP/MAS NMR spectra of samples prepared by forming small amounts (less than 0.1 equiv) of the  $\text{C}_7\text{H}_{11}^+$  cation in zeolite HZSM-5 and then absorbing an excess (typically 2 equiv) of the indicated base. Numbers in parentheses denote the experimental gas-phase proton affinities of the bases in units of kcal/mol. Adsorption of the weaker bases has no obvious effect on the  $\text{C}_7\text{H}_{11}^+$  cation, but the NMR spectra show that the stronger bases deprotonate the cation to form the neutral  $\text{C}_7\text{H}_{10}$  diene. All spectra were measured at 298 K, with the exception of acetone- $d_6$  which was measured at 193 K to prevent aldol condensation.

ion is clearly the energetically preferred state. Refinement of these predictions involves steric difficulties in fitting the larger onium ions in the zeolite channels, which we will discuss below.

In Table 1 we also present the calculated methyl cation affinities for all of the base molecules. There is little experimental data with which to judge the accuracy of the theoretical numbers. However, it is possible, using heats of formation and proton affinities,<sup>12</sup> to derive experimental methyl cation affinities ( $\Delta H$ ) for  $\text{H}_2\text{O}$  (66.6 kcal/mol),  $\text{CO}$  (78.3 kcal/mol), and  $\text{NH}_3$  (105.3 kcal/mol). These compare to calculated values of 73.9, 78.3, and 109.1 kcal/mol, which we consider reasonable agreement. Onium ion formation is predicted to be exothermic for every adsorbate with a  $\text{CH}_3^+$  affinity greater than or equal to that of  $\text{PH}_3$ , while no adsorbate with a  $\text{CH}_3^+$  affinity less than or equal to that of acetone is predicted to form an onium ion exothermically with  $\text{C}_7\text{H}_{11}^+$ . There is a fair correlation ( $R^2 = 0.8$ ) between the  $\text{CH}_3^+$  affinities and the binding energies of the onium complexes, although the bases bind to  $\text{CH}_3^+$  approximately 5 times stronger than they bind to  $\text{C}_7\text{H}_{11}^+$ .

**Experimental.** The key theoretical prediction was that coadsorption of a base with a proton affinity greater than 217 kcal/mol would deprotonate the  $\text{C}_7\text{H}_{11}^+$  carbenium ion in the zeolite to form the neutral  $\text{C}_7\text{H}_{10}$  cyclic diene. Figure 5 reports  $^{13}\text{C}$  CP/MAS spectra of zeolite HZSM-5 samples containing the  $\text{C}_7\text{H}_{11}^+$  cation and various adsorbed bases. The lower-most spectrum is a control experiment with no added base. This spectrum reveals the signature isotropic chemical shifts of this cation, 247, 148, 48, and 24 ppm; the full assignment of this spectrum is presented in Figure 6, which also reports GIAO-MP2 theoretical chemical shifts for this cation (modeled as a

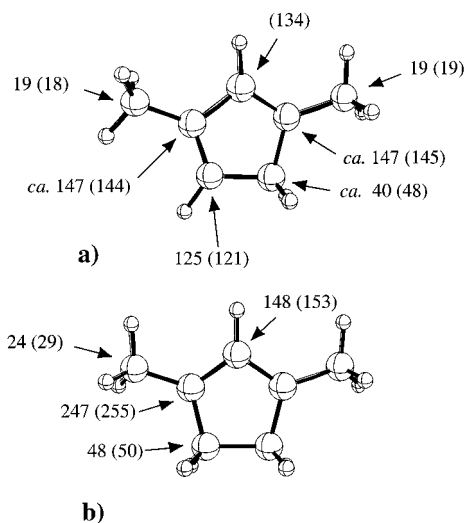


**Figure 6.** Experimental and theoretical (GIAO-MP2/tzp/dz//B3LYP/6-311G\*, in parentheses)  $^{13}\text{C}$  chemical shifts (ppm) for: (a)  $\text{C}_7\text{H}_{10}$  and (b)  $\text{C}_7\text{H}_{11}^+$ . Only symmetry-distinct atoms are annotated for  $\text{C}_7\text{H}_{11}^+$ . The resonance predicted by theory to be at 134 ppm in the spectrum of  $\text{C}_7\text{H}_{10}$  cannot be resolved in our experimental spectra as a result of the broad lines for this species in the zeolite and consequent spectral overlap.

gas-phase species) as well as for 1,3-dimethylcyclopenta-1,3-diene, the most stable olefin obtained by deprotonation of  $\text{C}_7\text{H}_{11}^+$ . As shown previously,<sup>8</sup> this level of theory consistently overestimates the  $^{13}\text{C}$  isotropic shifts of  $\text{C}_7\text{H}_{11}^+$  by approximately 5 ppm.

For the five examples of coadsorbed bases shown in Figure 5,  $^{13}\text{C}$  signals from the bases were minimized by the use of compounds with  $^{13}\text{C}$  levels found in nature, and in some cases also with deuterium substitution to further reduce the cross polarization signal intensity. It is clear from Figure 5 that nitromethane, acetone, and DMF, which all have proton affinities well below the deprotonation energy of  $\text{C}_7\text{H}_{11}^+$ , do not deprotonate the cation. However, coadsorption of the more basic pyridine has a profound effect: the  $\text{C}_7\text{H}_{11}^+$  cation is deprotonated. The most intense  $^{13}\text{C}$  signals observed following adsorption of pyridine are consistent with those of for 1,3-dimethylcyclopenta-1,3-diene (see Figure 6), and these assignments are also supported by dipolar dephasing experiments.  $^{13}\text{C}$  spectra obtained with coadsorbed pyridine invariably show a small signal at 86 ppm due to a minority product (vide infra). Adsorption of  $\text{P}(\text{CH}_3)_3$  almost quantitatively deprotonated the  $\text{C}_7\text{H}_{11}^+$  cation to 1,3-dimethylcyclopenta-1,3-diene, there was a very small amount of a second product (vide infra). The  $^{13}\text{C}$  signal at 5.9 ppm is due to  $\text{P}(\text{CH}_3)_3$ ; this is one of the more intense and better resolved signals from coadsorbed bases in Figure 5.

The results in Figure 5 experimentally bracket the enthalpy of deprotonation of the  $\text{C}_7\text{H}_{11}^+$  cation between 212 and 222 kcal/mol. Coadsorption of DMA (Exp. PA = 217 kcal/mol) helps to narrow these limits. Figure 7 shows that coadsorption of 1 equiv of DMA has little if any effect on the  $\text{C}_7\text{H}_{11}^+$  cation, but a higher loading, 2 equiv, deprotonates some of the cation to form the diene. From this result, we conclude that the deprotonation enthalpy of the  $\text{C}_7\text{H}_{11}^+$  cation is slightly greater than 217 kcal/mol, very close to the best theoretical value of 215.6 kcal/mol.

Figure 8 reveals that some, but not all, of the  $\text{C}_7\text{H}_{11}^+$  cations are deprotonated by the first 0.5 equiv of pyridine. Since the yield of the  $\text{C}_7\text{H}_{11}^+$  cation prepared by the method used here

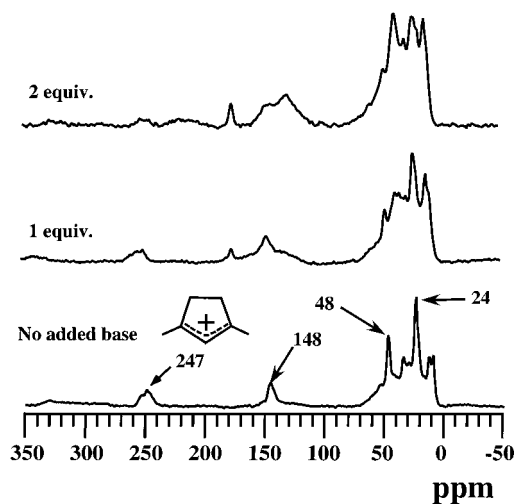


**Figure 7.**  $^{13}\text{C}$  CP/MAS NMR spectra of samples prepared by forming small amounts (less than 0.05 equiv) of the  $\text{C}_7\text{H}_{11}^+$  cation in zeolite HZSM-5 and then absorbing 0, 1, or 2 equiv of dimethylacetamide (DMA). Deprotonation of the  $\text{C}_7\text{H}_{11}^+$  cation occurs with 2, but not 1, equiv of DMA. All spectra were measured at 298 K.

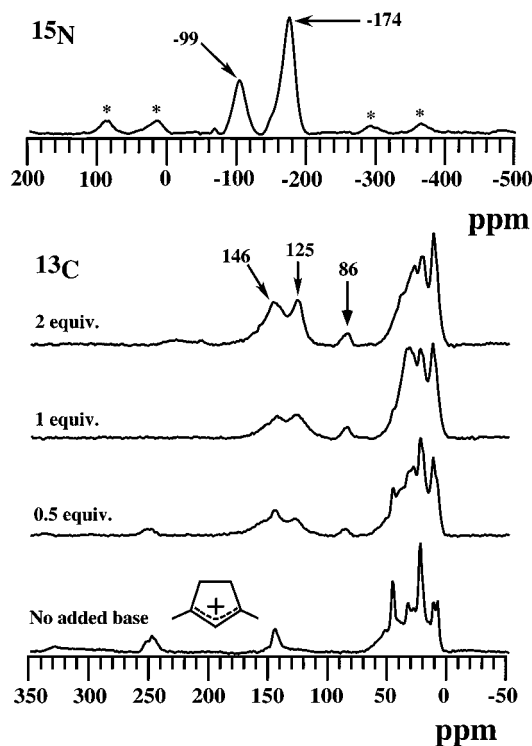


**Figure 8.** CP/MAS NMR spectra of samples prepared by forming small amounts (less than 0.05 equiv) of the  $\text{C}_7\text{H}_{11}^+$  cation in zeolite HZSM-5 and then absorbing the indicated amounts of pyridine (Py)- $^{15}\text{N}$ .  $^{13}\text{C}$  spectra are shown for several loadings and an  $^{15}\text{N}$  spectrum is shown for the 2-equiv sample. The 86 ppm resonance due to a small amount of the pyridinium complex of the  $\text{C}_7\text{H}_{11}^+$  cation,  $\text{C}_7\text{H}_{11}\text{Py}^+$ , is indicated in the  $^{13}\text{C}$  spectra. This species is not resolved in the  $^{15}\text{N}$  spectrum which shows a signal at  $-174$  ppm due to pyridine protonated by Brønsted sites in the zeolite and a signal at  $-99$  ppm due to pyridine on Lewis sites in the catalyst binder. All  $^{13}\text{C}$  spectra were measured at 298 K, and the  $^{15}\text{N}$  spectrum was measured at 123 K.

typically corresponds to 0.01–0.04 equiv of all Brønsted sites of the zeolite, this suggests that not all Brønsted sites are equally preferred as adsorption sites. No  $\text{C}_7\text{H}_{11}^+$  cation remains after adsorption of a full equivalent of pyridine. The  $^{13}\text{C}$  signal at 86 ppm, which reproducibly forms when pyridine reacts with the

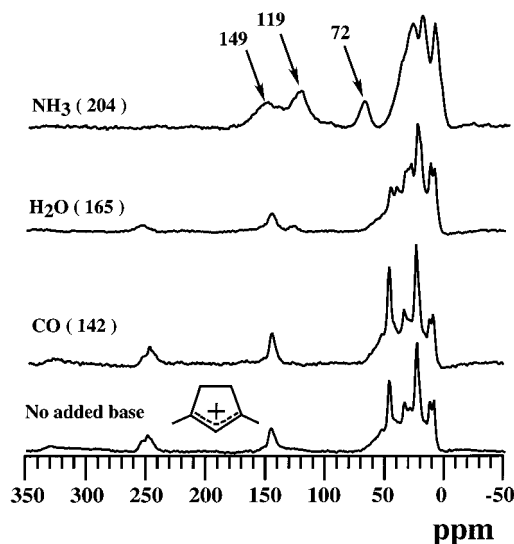


**Figure 9.**  $^{13}\text{C}$  CP/MAS NMR spectra of samples prepared by forming small amounts (less than 0.05 equiv) of the  $\text{C}_7\text{H}_{11}^+$  cation in zeolite HZSM-5 and then absorbing an excess (typically 2 equiv) of the indicated base. Numbers in parentheses denote the experimental gas-phase proton affinities of the bases in units of kcal/mol. The 72 ppm signal from the ammonium complex of  $\text{C}_7\text{H}_{11}^+$ ,  $\text{C}_7\text{H}_{11}\text{NH}_3^+$ , is indicated for the spectrum of the sample prepared by coadsorption of ammonia. As a result of the use of cross polarization, physisorbed CO is not seen in the spectrum of the sample prepared with this coadsorbate. All spectra were measured at 298 K.

$\text{C}_7\text{H}_{11}^+$  cation in zeolite HZSM-5, is a minority reaction product which is assigned following presentation of the results for coadsorbed ammonia. The  $^{15}\text{N}$  CP/MAS spectrum in Figure 8 shows that pyridine is protonated in the zeolite ( $-174$  ppm). The  $^{15}\text{N}$  signal at  $-99$  ppm corresponds to pyridine adsorbed at Lewis sites on the alumina binder used to pelletize the zeolite powder.

Figure 9 reports  $^{13}\text{C}$  CP/MAS spectra of samples prepared following adsorption of three weak bases,  $\text{H}_2\text{O}$ ,  $\text{CO}$ , and  $\text{NH}_3$ , that, on the basis of analogous reactions in solution media, could conceivably react with the  $\text{C}_7\text{H}_{11}^+$  cation as nucleophiles. Water (Exp. PA = 166 kcal/mol for the monomer) is too weakly basic to deprotonate the cation; if it acted as a nucleophile, a hydroxonium cation would be produced. From Figure 9 it is clear that neither reaction occurs. Oxonium ions were also not observed upon adsorption of either methanol or DME using a pulse quench reactor.

Alkyl carbenium ions in superacid media can react with  $\text{CO}$  (Exp. PA = 142 kcal/mol) to form acylium cations.<sup>22</sup> Figure 9 shows a representative attempt to convert the  $\text{C}_7\text{H}_{11}^+$  cation into an acylium ion in the zeolite; in this case  $^{13}\text{CO}$  was cryopumped onto the zeolite (containing the cation) at 77 K and 40 Torr. In every case, a modest amount of  $\text{CO}$  was physisorbed by the zeolite to yield a peak at 190 ppm in Bloch decay spectra (not shown), but no reaction products were observed. Binding of  $\text{CO}$  to the  $\text{C}_7\text{H}_{11}^+$  cation was also not observed when the sample was cooled to  $\sim 123$  K in the NMR probe and acylium ions also did not form upon sample heating in the probe. We consider the experimental finding that the  $\text{C}_7\text{H}_{11}^+$  cation does not bind  $\text{CO}$  in zeolite HZSM-5 to form an acylium ion to be unequivocal, completely in line with our theoretical predictions.

(22) Xu, T.; Barich, D. H.; Torres, P. D.; Nicholas, J. B.; Haw, J. F. J. *Am. Chem. Soc.* **1997**, *119*, 396–405.

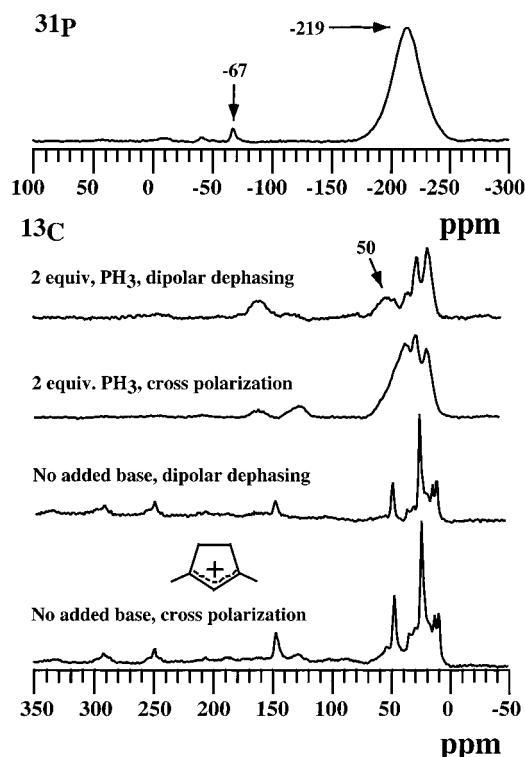


**Figure 10.** CP/MAS NMR spectra of samples prepared by forming small amounts (less than 0.05 equiv) of the  $C_7H_{11}^+$  cation in zeolite HZSM-5 and then absorbing the indicated amounts of phosphine,  $PH_3$ .  $^{13}C$  spectra are shown for 0- and 2-equiv samples, and a  $^{31}P$  spectrum is shown for the 2-equiv sample. The 44-ppm resonance due to the phosphorus-substituted quaternary carbon of the phosphonium complex of  $C_7H_{11}^+$ ,  $C_7H_{11}PH_3^+$ , is clearly resolved in a  $^{13}C$  spectrum measured with dipolar dephasing. This species is also observed at  $-67$  ppm in the  $^{31}P$  spectrum which also shows a signal at  $-219$  ppm due to phosphine adsorbed in the zeolite. All spectra were measured at 298 K.

In contrast, the  $C_7H_{11}^+$  cation reacted quantitatively with  $NH_3$  (Exp. PA = 204.0 kcal/mol) to form a new species,  $C_7H_{11}NH_3^+$ , with a distinctive  $^{13}C$  resonance at 72 ppm, exactly where one would expect to find a tertiary carbon bound to an ammonium ( $-NH_3^+$ ) group. This spectrum is assigned to species shown in Figure 1c. Recall that adsorption of pyridine converted a minor amount of the  $C_7H_{11}^+$  cation into a species with a  $^{13}C$  shift of 86 ppm. By analogy to ammonium species, the minority reaction product with pyridine is assigned to the pyridinium ion  $C_7H_{11}-Py^+$  shown in Figure 4c.

$PH_3$ , with an experimental proton affinity of 188 kcal/mol, is much less basic than  $NH_3$ , and Figure 10 shows that the  $C_7H_{11}^+$  cation is not deprotonated by this base. The  $^{13}C$  resonance for the carbon bonded to phosphorus is at 50 ppm, and is poorly resolved from signals due to the other carbons in the complex. We resolved this signal using a dipolar dephasing (interrupted decoupling) pulse sequence at reduced temperature (Figure 10). Further evidence for assignment to  $C_7H_{11}PH_3^+$  was a  $^{31}P$  resonance at  $-67$  ppm. The dominant signal in the  $^{31}P$  spectrum, at  $-219$  ppm, is due to unreacted  $PH_3$  hydrogen-bonded to Brønsted sites on the catalyst. By a similar procedure we were able to determine that  $P(CH_3)_3$  does indeed form a phosphonium complex,  $C_7H_{11}P(CH_3)_3^+$  with the  $C_7H_{11}^+$  cation as a minority product (not shown). In this case, steric constraints prevent complete reaction, and deprotonation to form the neutral diene is the preferred pathway in the zeolite.

## Discussion

Excellent agreement between experimental results and theoretical predictions was obtained for a wide variety of coadsorbed bases. The B3LYP/6-311G\* calculations correctly predicted the equilibrium state of the carbenium ion and each coadsorbed base. The only complication is the known overestimation of the deprotonation enthalpy of  $C_7H_{11}^+$  at the B3LYP/6-311G\* level of theory.

Weaker bases such as CO,  $H_2O$ , nitromethane, DME, acetone, and DMF neither deprotonated  $C_7H_{11}^+$  nor reacted with it to form an onium ion. Rather, they formed hydrogen-bonded complexes. In contrast, coadsorption of the strong bases pyridine and  $P(CH_3)_3$  into the zeolite deprotonated the  $C_7H_{11}^+$  cation to form the neutral cyclic diene, 1,3-dimethylcyclopenta-1,3-diene. In a recent study of the mechanism of methanol to hydrocarbon catalysis,<sup>8</sup> we showed that (in the absence of a coadsorbate) the adsorption complex of this neutral diene on a zeolite Brønsted site was only 2 kcal/mol less stable than the ion pair of the  $C_7H_{11}^+$  cation and the conjugate base of the Brønsted site. We proposed that the higher-energy state was thermally accessible under reaction conditions and that the neutral diene was methylated as one of a sequence of steps in a catalytic cycle by which methanol was converted to olefins. Neutral 1,3-dimethylcyclopenta-1,3-diene was not observed experimentally in that investigation. The observation here, that 1,3-dimethylcyclopenta-1,3-diene is liberated on the zeolite by a stronger base, does not prove that cyclic dienes are involved in the mechanism of hydrocarbon synthesis from methanol. However, had the opposite result been obtained, that the  $C_7H_{11}^+$  cation formed irreversibly on the zeolite and could not be deprotonated, the proposed mechanism would have been undermined.

Coadsorption of DMA is a particularly interesting case. Using a combination of NMR and theoretical methods, we recently showed that the degree of proton transfer from a zeolite Brønsted site to acetone was increased by the coadsorption of nitromethane or similar weak bases.<sup>23</sup> Our theoretical calculations<sup>24</sup> indicate that the interaction between coadsorbates and acetone increases acetone's proton affinity, thus promoting proton transfer. In this study, coadsorption of 1 equiv of DMA did not appear to deprotonate  $C_7H_{11}^+$ , while 2 equiv did result in some deprotonation. As expected, at higher loading there is also an effective increase in the basicity of DMA due to the interaction with neighboring molecules, which promotes deprotonation of the carbenium ion, an independent demonstration of the previously reported solvent effect in zeolite catalysis.

In this study we theoretically obtained geometries for 11  $C_7H_{11}^+ \cdots B$  complexes with C-H  $\cdots X$  hydrogen bonds (Figure 1a and Figure 2). Most previously observed C-H  $\cdots O$  hydrogen bonds are quite weak, giving (absolute) binding energies of less than 4 kcal/mol.<sup>1</sup> In this study we obtain much stronger binding energies that range from  $-10.3$  to  $-17.6$  kcal/mol. The very strong nature of these hydrogen bonds is clearly related to the very high acidity of the carbenium proton. Vargas et al.<sup>25</sup> proposed that the relationship between the C-H  $\cdots O$  hydrogen bond strength and the deprotonation enthalpy of the C-H proton is linear;  $D_e = 0.0551(\Delta H_{\text{deprot}}) - 23.6$  (values in kcal/mol). From this relationship and our calculated deprotonation enthalpy for  $C_7H_{11}^+$ , we can predict a hydrogen bond enthalpy of  $-11.7$  kcal/mol. This value is similar to our

(23) Haw, J. F.; Xu, T.; Nicholas, J. B.; Goguen, P. W. *Nature* **1997**, *389*, 832–835.

(24) Nicholas, J. B. *Top. Catal.* **1999**, *9*(3–4), 181–189.

(25) Vargas, R.; Garza, J.; Dixon, D. A.; Hay, B. P. *J. Am. Chem. Soc.* **2000**, *104*, 5115–5121.



calculated binding energy for the  $C_7H_{11}^+ \cdots H_2O$  complex ( $-12.6$  kcal/mol). There does not appear to be a well-defined trend in the binding energies for the C–H  $\cdots$  O bonds formed by all of the bases, although as the difference between the proton affinity of the base and the deprotonation enthalpy of  $C_7H_{11}^+$  becomes less, the binding energy tends to increase. Less commonly observed are C–H  $\cdots$  N hydrogen bonds,<sup>1</sup> as exhibited in the  $NH_3$  and pyridine complexes. These also are generally assumed to be very weak interactions ( $<4$  kcal/mol), whereas our complexes are strongly bound ( $-12.2$  kcal/mol for  $NH_3$  and  $-11.1$  kcal/mol for pyridine). Even more unusual are the C–H  $\cdots$  C hydrogen bond in the CO complex, and the two C–H  $\cdots$  P hydrogen bonds in the  $PH_3$  and  $P(CH_3)_3$  complexes. Not surprisingly, the C–H  $\cdots$  C hydrogen bond is quite weak ( $-2.2$  kcal/mol), as the carbon in CO is very weakly basic. The C–H  $\cdots$  P hydrogen bonds are relatively weak in comparison to those involving oxygen as an acceptor, despite the relatively high proton affinities of the bases. This may be due to the high s character of the lone pair on phosphorus, and thus its unavailability for hydrogen bonding.<sup>26</sup> We are not aware of any previous experimental reports of C–H  $\cdots$  C or C–H  $\cdots$  P hydrogen bonds.

We were also able to theoretically obtain stable geometries for six complexes which have  $\pi$ -cation interactions between the olefin double bond and the acidic proton of the protonated bases. The weak basicity of  $PH_3$  results in a high energy  $C_7H_{10} \cdots PH_4^+$  complex that certainly does not exist under experimental conditions. However, formation of the other five complexes is exothermic, with values ranging from  $-6.3$  to  $-15.0$  kcal/mol below the sum of the total energies of the isolated reactants. These binding energies are quite reasonable. For example, the  $\pi$ -cation binding energy between  $Na^+$  and ethylene is  $\sim -13.6$  kcal/mol.<sup>27</sup>

Onium ions were observed experimentally in every case for which theory predicted these to be the most stable states. For reaction with  $NH_3$  and  $PH_3$  experiment verified that the onium ions were the major products. Onium ions were minority products with pyridine and  $P(CH_3)_3$ . However, these are very large ions. Given that the channels of HZSM-5 are only  $\sim 5.5$  Å in diameter, accommodation of bulky onium ions such as shown in Figure 4c and d will be difficult, even in the more spacious channel intersections. We did not seek to model the effect of zeolite framework topology on the accessibility of the three states.

(26) a. Dixon, D. A.; Dunning, T. H., Jr.; Eades, R. A.; Gassman, P. G. *J. Am. Chem. Soc.* **1983**, *105*, 7011; b. Cherry, W.; Epiotis, N. D. *J. Am. Chem. Soc.* **1976**, *98*, 1135.

(27) Feller, D. *Chem. Phys. Lett.* **2000**, *322*, 543–548.

A fundamental concern in efforts to quantify the acid or base strengths of surfaces is that if adsorption of probe molecules occurs irreversibly, thermodynamic equilibrium will not be established. Here we saw that the reactions between the carbenium ion and coadsorbed bases went to equilibrium in the zeolite, with the position of equilibrium being that predicted by gas-phase thermochemical properties. Implicit in the notion of reversibility is the time scale of the measurement, which was quite slow in this case, but not slower than other spectroscopy-based methods for evaluating the strengths of solid acids.

## Conclusions

Our recent theoretical approach for predicting which carbenium ions will be persistent species in acidic zeolites has been validated experimentally by showing that  $C_7H_{11}^+$  is deprotonated to form the  $C_7H_{10}$  cyclic diene by a base with gas-phase proton affinity greater than the calculated deprotonation enthalpy (215.6 kcal/mol) of  $C_7H_{11}^+$ . Extensions of this theoretical approach also made a number of specific predictions about onium ion formation with a number of bases. These predictions were verified experimentally with the caveat that bulky ions such as those formed between  $C_7H_{11}^+$  and pyridine and  $P(CH_3)_3$  (Figure 4c and d) were minority products due to steric constraints in the zeolite. Although phosphonium and ammonium ion formation was quantitative for  $PH_3$  and  $NH_3$ , respectively, no acylium cation was obtained with CO, and no oxonium ion was obtained with  $H_2O$ —all in agreement with theoretical predictions. We also obtained theoretical geometries for several complexes that exhibit unusual C–H  $\cdots$  X hydrogen bonds.

**Acknowledgment.** We thank David A. Dixon for helpful discussions. J.F.H. is supported by the National Science Foundation (CHE-9996109) and the U.S. Department of Energy (DOE) Office of Basic Energy Sciences (BES) (Grant No. DE-FG03-93ER14354). J.B.N. is funded by the Department of Energy (DOE) Office of Science. Computer resources were provided by the National Energy Research Supercomputer Center (NERSC), Berkeley, CA, the Molecular Science Computing Facility (MSCF) at PNNL, and the National Center for Supercomputing Applications (NCSA). The MSCF is operated with funds provided by DOE's Office of Biological and Environmental Research. Pacific Northwest National Laboratory is a multipurpose national laboratory operated by Battelle Memorial Institute for the U.S. DOE.

JA002775D